

INFRARED TIME LAGS FOR THE PERIODIC QUASAR PG 1302-102

HYUNSUNG D. JUN^{1,2}, DANIEL STERN¹, MATTHEW J. GRAHAM³, S. G. DJORGOVSKI³, AMY MAINZER¹, ROC M. CUTRI⁴,
ANDREW J. DRAKE³ & ASHISH A. MAHABAL³

Re-Submitted Version — 2015 October 16

ABSTRACT

The optical light curve of the quasar PG 1302-102 at $z = 0.278$ shows a strong, smooth 5.2 yr periodic signal, detectable over a period of ~ 20 yr. Although the interpretation of this phenomenon is still uncertain, the most plausible mechanisms involve a binary system of two supermassive black holes with a subparsec separation. At this close separation, the nuclear black holes in PG 1302-102 will likely merge within $\sim 10^5$ yr due to gravitational wave emission alone. Here we report the rest-frame near-infrared time lags for PG 1302-102. Compiling data from *WISE* and *Akari*, we confirm that the periodic behavior reported in the optical light curve from Graham et al. (2015a) is reproduced at infrared wavelengths, with best-fit observed-frame 3.4 and $4.6\mu\text{m}$ time lags of $(2219 \pm 153, 2408 \pm 148)$ days for a near face-on orientation of the torus, or $(4103 \pm 153, 4292 \pm 148)$ days for an inclined system with relativistic Doppler boosting in effect. The periodicity in the infrared light curves and the light-travel time of the accretion disk photons to reach the dust glowing regions support that a source within the accretion disk is responsible for the optical variability of PG 1302-102, echoed at the further out dusty regions. The implied distance of this dusty, assumed toroidal region is ~ 1.5 pc for a near face-on geometry, or ~ 1.1 pc for the relativistic Doppler boosted case.

Subject headings: galaxies: active — quasars: individual (PG 1302-102)

1. INTRODUCTION

Optical reverberation mapping, measuring the time delay between variations in the accretion disk optical continuum luminosity of an active galactic nucleus (AGN) and the delayed response of the broad emission line luminosity, has become a standard technique to study the physics and structure of the inner regions of AGN (e.g., Blandford & Payne 1982; Peterson 1993; Bentz et al. 2006). Such studies enable measurement of the physical size of the broad line region, opening a way to estimate the virial black hole masses of distant AGNs (e.g., McLure & Jarvis 2002; Vestergaard & Peterson 2006; Jun et al. 2015) through the relation between broad line region size and optical luminosity ($R_{\text{BLR}} \sim L^{0.5}$; e.g., Kaspi et al. 2000; Bentz et al. 2006).

Analogous to optical broad line reverberation analyses, light travel time lags between the ultraviolet/optical and near-infrared continuum provide a measurement of the physical size of the infrared-emitting dusty tori that are believed to surround most AGN (e.g., Penston et al. 1974; Clavel et al. 1989; Suganuma et al. 2006). The inferred time-lag-based sizes from this dust reverberation, supported by direct interferometric K -band measurements for a few nearby AGN (e.g., Swain et al. 2003; Kishimoto et al. 2011a), shows that the dust emitting region scales with the ultraviolet/optical luminosity ($R_{\text{dust}} - L$ relation; e.g., Oknyanskij & Horne 2001; Koshida et al. 2014) with a similar square root power as the $R_{\text{BLR}} - L$ relation, but with a larger normalization. These radius-luminosity relations indicate that the geometric components of an AGN are spatially structured, such that illumi-

nation of the accretion disk propagates first through the broad line and later through the cooler, dusty regions.

Recently, Graham et al. (2015a) reported an unusual example of an optically variable quasar, PG 1302-102 at $z = 0.278$. The 9-yr optical light curve from the Catalina Real-time Transient Survey (CRTS; Drake et al. 2009), combined with historical data going back ~ 20 yrs, shows periodic variability with an observed period of 1884 ± 88 days. Additional examples of similarly periodic quasars have recently been reported by Graham et al. (2015b) and Liu et al. (2015). This unusual phenomenology is distinct from the typical variability of most quasars which is akin to a damped random walk (e.g., MacLeod et al. 2012; Graham et al. 2014). The most likely interpretations of the periodic quasars involve close, subparsec binary supermassive black hole systems (e.g., D’Orazio et al. 2015a,b; Graham et al. 2015b).

Taking advantage of the distinct periodic signals in the optical, we investigate the infrared light curves of PG 1302-102 using data from the *Wide-field Infrared Survey Explorer* (*WISE*; Wright et al. 2010) and *Akari* (Murakami et al. 2007) missions. We also include more recent data from the *Near-Earth Object WISE Reactivation* mission (*NEOWISE-R*; Mainzer et al. 2014). We measure the time lags between the optical and infrared emission, thereby confirming that the optical periodicity is reproduced in the dust emission and provides a size measurement of the dust-emitting region. Furthermore, using multi-band $3.4\mu\text{m}$ ($W1$) and $4.6\mu\text{m}$ ($W2$) data, we investigate wavelength-dependent trends in the light curve time delays, which provide further information about the size and structure of the dusty torus. In a separate, related paper, D’Orazio et al. (2015b) report on the UV light curve of PG 1302-102, showing that it is consistent with relativistic boosting from a supermassive black hole binary being the cause of the observed UV and optical periodicity.

In this *Letter*, we describe the data collection and processing in §2, the measurement of time-lags and amplitudes in §3, and their implication for the binary supermassive black hole

¹Jet Propulsion Laboratory, California Institute of Technology, 4800 Oak Grove Drive, Pasadena, CA 91109, USA [e-mail: hyunsung.jun@jpl.nasa.gov]

²NASA Postdoctoral Program Fellow

³California Institute of Technology, 1216 E. California Blvd., Pasadena, CA 91125, USA

⁴Infrared Processing and Analysis Center, California Institute of Technology, Pasadena, CA 91125, USA

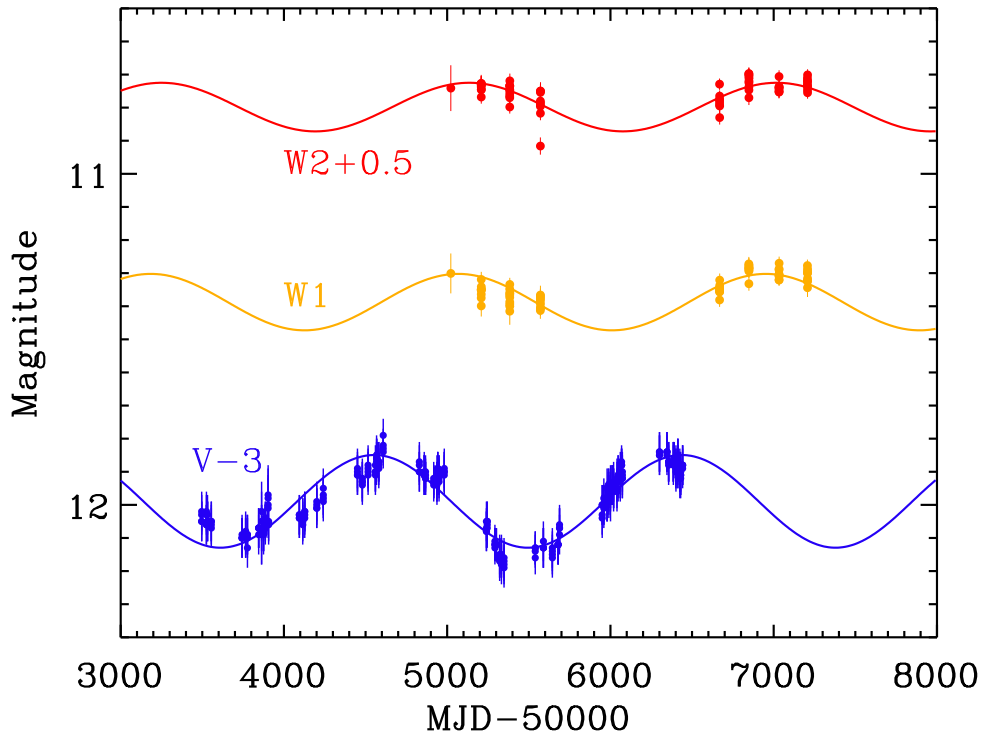


Figure 1. The light curves for PG 1302-102 in CRTS optical (blue), *WISE/NEOWISE-R* *W1* (yellow), and *W2* (red). The earliest *W1* and *W2* magnitudes are derived from the *Akari* 2.5 – 5.0 μ m grism spectra (§2). Overplotted sinusoids are the best-fit curves from Graham et al. (2015a) and this work (§3), in the same colors as each data.

interpretation in §4. Throughout, photometry is reported in the Vega system and we adopt a flat Λ CDM cosmology with $H_0 = 70 \text{ km s}^{-1} \text{ Mpc}^{-1}$, $\Omega_m = 0.3$ and $\Omega_\Lambda = 0.7$.

2. MID-INFRARED OBSERVATIONS

PG 1302-102 is bright enough to have been detected in single exposures throughout the *WISE* mission. Collecting both cryogenic and post-cryogenic multi-epoch photometry from the AllWISE and *NEOWISE-R* data releases, as well as the most recent (pre-release) *NEOWISE-R* observations of PG 1302-102, we measure *W1* and *W2* light curves spanning 5.5 years (MJD 55208-57207). The data consist of seven groups spaced at intervals of roughly six months, albeit with a three year gap when *WISE* was in hibernation (MJD 55572-56668). Each group has 10-15 observations, with the latest data taken in July 2015. *NEOWISE-R* is expected to obtain ~ 3 additional groups of observations over the next ~ 1.5 yrs. We do not include longer wavelength data at 12 μ m (*W3*) or 22 μ m (*W4*) which are restricted to the cryogenic period of the *WISE* mission as the temporal coverage of those observations consist of only two groups. We further removed the data suffering from bad quality frames (*qual_frame=0*), charged particle hits (*saa_sep<0*), or scattered moonlight (*moon_masked=1*).

Supplementing the *WISE* observations of PG 1302-102, we also analyzed archival 2.5 – 5.0 μ m grism spectra obtained by *Akari* six months prior to the *WISE* observations (Ohyama et al. 2007). Out of three post-cryogenic *Akari* spectra of PG 1302-102 taken on MJD 55022-55023, we removed the second spectrum as it is significantly affected by hot pixels. We convolved the processed and extracted spectra from the other two observations with the *WISE* filter responses (Wright et al. 2010) to obtain *W1* and *W2* equivalent magnitudes. Because the *W2* filter response extends longward of 5 μ m, the wavelength cutoff of post-cryogenic *Akari*, we ex-

trapolated the spectrum redward based on a power law fit, taking into account the 1σ uncertainties in the fitted parameters. Finally, we averaged the two *Akari* magnitudes, separated by one day, to improve the sensitivity. For ease of description, in the following we discuss the *W1* and *W2* light curves, though those light curves also include these earlier epoch *Akari* observations. Figure 1 presents the CRTS, *WISE*, and *Akari* light curves with the periodic functional fits (§3) overplotted.

3. MEASUREMENT OF THE TIME LAGS

Assuming that the optical variability of PG 1302-102 arises from the accretion disk(s) of the (binary) AGN, we expect the fluctuations in the optical luminosity to process through the inner dusty torus and produce a distribution of time lags in the hot dust emission corresponding to the light travel time to the inner portions of the torus. We aim to measure the cross-correlation signal between the optical and infrared magnitudes, and test if the infrared light curves trace the periodic variability appearing in the optical time series data.

Because the optical light curves in Graham et al. (2015a) show a well defined periodic behavior, we first cross correlate their sinusoidal model fit with the *W1* and *W2* band data. In Figure 2(a) we plot the cross correlation amplitudes for a range of time lags. The cross correlation amplitudes peak at 0.69 for *W1* and 0.63 for *W2*, indicating that the *WISE* data are moderately correlated to the periodic optical light curve model.

To give proper treatment of the uncertainties into the cross correlation analysis (e.g., Peterson et al. 1998), we performed a set of Monte Carlo simulations including the observational uncertainty from the CRTS data (0.06 mag) and the uncertainty in the optical period (88 days). We performed 100,000 realizations adding random Gaussians to the model magnitudes with $\sigma = 0.06$ mag, and modifying the period by adding random Gaussians with $\sigma = 88$ days. We measured the cen-

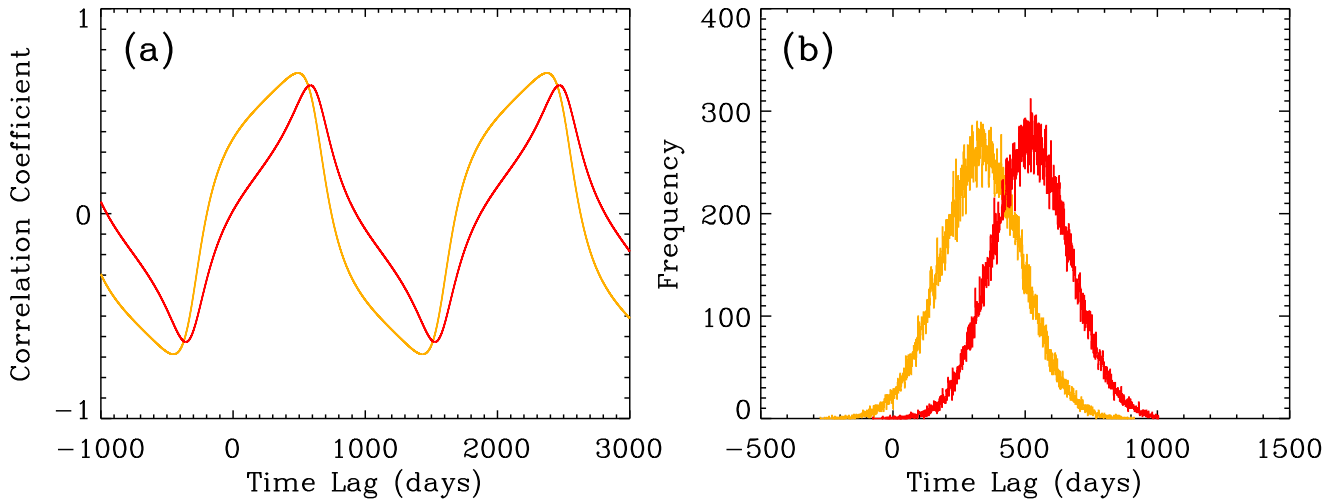


Figure 2. (a) The cross correlation amplitudes for PG 1302-102 between the best-fit optical model and the *WISE* *W1* (yellow) and *W2* (red). (b) Monte Carlo simulation of the time lags for *W1* (yellow) and *W2* (red) taking into account the uncertainties in the observed magnitudes and period.

triod of each simulated cross correlation function where the amplitudes were above 0.8 times the peak value, while limiting the range of time lags to $[-500, 1500]$ days to do away with the other periodic solutions. In Figure 2(b) we plot the resultant distribution of the time lags from the Monte Carlo simulations. Adopting the fiducial time lag as the mean of the distribution of simulated time lags, and the uncertainty as the 34.13% percentile in the time lag distribution deviated from the mean (Peterson et al. 1998), the *W1* and *W2* time lags to the optical model (τ , observed-frame days) become

$$\begin{aligned} \tau_{W1} &= (335 \pm 153) + 1884n \\ \tau_{W2} &= (524 \pm 148) + 1884n \end{aligned} \quad (1)$$

with any integer ($n = 0, \pm 1, \pm 2, \dots$) multiples of 1884 days providing equally probable solutions (at least mathematically, if not physically).

The sizable cross correlation amplitudes to the periodic model imply that the *WISE* light curves are also periodically variable. We checked this by fitting the infrared light curves of PG 1302-102 with periodic functions and calculating the signal-to-noise (S/N) of the periodic modulation above white noise. Adopting the sinusoidal period from Graham et al. (2015a), we fit the magnitude $m(t)$ at the observed-frame time t as $m(t) = A \cos(2\pi t/T) + B$, solving for amplitude A and magnitude zero-point B , and fixing the period $T = 1884$ days. Applying the best-fit values into the periodic S/N ratio indicator of Horne & Baliunas (1986), we get values of 5.7, 4.1, and 3.4 in the optical, *W1*, and *W2*, respectively. The false alarm probability F that a periodicity in the data arises from pure noise, equations (13) and (23) from Horne & Baliunas (1986), yield $F \sim 3 \times 10^{-50}$ from the CRTS data alone, and $\sim 4 \times 10^{-10}$ and $\sim 1 \times 10^{-9}$ for *W1* and *W2*, where these estimates of F were calculated assuming evenly spaced data. The extremely small F values imply with high likelihood that the source is periodic in all three wavebands.

We next attempt to estimate the most reasonable time lag between the optical and mid-infrared light curves, τ in equation (1), out of the infinite number of solutions allowed. First, we assume that the time lags are positive such that they represent the reverberation of the incident optical photons through dust re-processed emission, requiring $n \geq 0$ in equation (1).

Further refinement of the value of n requires a physical

model of the system. In the general picture of a toroidally shaped dusty torus, most of the mid-infrared emission at these wavelengths will come from the inner edge of the torus, with longer wavelength emission coming from slightly larger radii, corresponding to cooler material (e.g., Nenkova et al. 2008). For an axisymmetric model of the torus simply responding to variations in the accretion disk luminosity, the time delay then depends on the light travel time to the inner edge of the torus and the orientation of the torus relative to our line of sight, $\tau = R(1 + \sin i)/c$, where R is the radius of the inner edge of the torus, c is the speed of light, and i is the inclination angle ($i = 0^\circ$ corresponds to face-on; $i = 90^\circ$ corresponds to edge-on). Alternatively, D’Orazio et al. (2015b) present a compelling and physically motivated model for PG 1302-102 where the modulated UV/optical emission is due to relativistic Doppler boosting of emission from a “minidisk” in a steadily accreting, unequal mass binary. In 2D and 3D hydrodynamical simulations of supermassive black hole binaries, circumprimary and circumsecondary minidisk accretion flows form around the two black holes, with a larger circumbinary accretion disk on larger scales (e.g., Shi et al. 2012; D’Orazio et al. 2013). For an unequal mass system, the secondary carves out an annular region in the circumbinary disk, limiting the amount of material that reaches the primary. Most of the emission at optical through X-ray energies will thus be associated with the rapidly accreting secondary, which D’Orazio et al. (2015b) show is likely moving at $\sim 0.07c$ with an orbital inclination of $i = 60 - 90^\circ$ for the PG 1302-102 system. Relativistic Doppler boosting then produces a system akin to a rotating lighthouse, producing a sinusoidal light curve with a period T . Whereas the peaks of the UV and optical light occur when the “lighthouse” is pointed towards the observers line-of-sight, peaks in the thermal mid-infrared emission, which is predominantly coming from the inner wall of the far side of the torus, correspond to when the “lighthouse” is pointed away from the observer, giving an additional $T/2$ to the infrared time lag.

We can now use these models to place limits on the dust lags based on the sublimation radius of hot dust. The physically motivated lighthouse model is effective when the inclination is large so that the relativistic boosting is working, and the near side of the torus is blocked from our line of sight. Thus, our variable circumbinary accretion disk

model predicts $\tau = R(1 + \sin i)/c$ and is appropriate for small i , while the relativistic Doppler boosting model predicts $\tau = R(1 + \sin i)/c + T/2$ and requires large i . The inner radius of the torus corresponds to the dust sublimation radius R_{sub} , i.e., the closest distance to the central engine that dust is not destroyed, and we solve for n in the $W1$ time lag from equation (1) where the two radii are closest to each other, or $R \simeq R_{\text{sub}}$. Graphite dust grains are better able to survive in the hotter, inner region of the torus than silicate, and they are thought to be responsible for the rest-frame near-infrared emission from quasars (e.g., Mor & Netzer 2012; Jun & Im 2013). We use the graphite dust sublimation radius $R_{\text{sub}} \simeq 0.5(L_{\text{bol}}/10^{46} \text{ erg s}^{-1})^{0.5} \text{ pc}$ for a sublimation temperature $T_{\text{sub}} = 1800 \text{ K}$ (Mor & Netzer 2012). At $z = 0.278$ and a median $V \simeq R \simeq 15.0 \text{ mag}$ for PG 1302-102 (Marziani et al. 1996; Ojha et al. 2009; Prochaska et al. 2011; Graham et al. 2015a), $L_{\text{bol}} \simeq 6.78 \times 10^{46} \text{ erg s}^{-1}$ adopting a 5100\AA to bolometric correction of 10.33 (Richards et al. 2006). Thus, we have $R_{\text{sub}} \simeq 1550$ rest-frame light days (1.30 pc), or $R_{\text{sub}} \simeq 1980$ observed-frame light days. For a near face-on orientation of the torus ($i \simeq 0^\circ$), $\tau = R(1 + \sin i)/c \simeq R/c$ and the $n = 1$ solution from equation (1), $(\tau_{W1}, \tau_{W2}) = (2219 \pm 153, 2408 \pm 148)$ days, best meets $R \simeq R_{\text{sub}}$ from the $W1$ time lag, with $R = 1.12R_{\text{sub}} = 1.46 \text{ pc}$. Meanwhile, for a relativistic Doppler boosted torus with $i = 60 - 90^\circ$, the $n = 2$ solution, $(\tau_{W1}, \tau_{W2}) = (4103 \pm 153, 4292 \pm 148)$ days, gives the best match between R and R_{sub} with $R = 0.80 - 0.86R_{\text{sub}} = 1.04 - 1.11 \text{ pc}$. We note that the uncertainty in the $R \simeq R_{\text{sub}}$ approximation could be a few tens of percent (Mor & Netzer 2012), and that even with the same adopted $T_{\text{sub}} = 1800 \text{ K}$, the value of R_{sub} varies across the literature by 20-60% due to slightly different model assumptions (e.g., Barvainis 1987; Nenkova et al. 2008). Also the uncertainty in the bolometric correction from the mean quasar template could be as large as 50% (Richards et al. 2006), translating into 25% uncertainty in R_{sub} .

We now consider the most probable *WISE* time lags in the context of the observed $R_{\text{dust}} - L$ relation from Koshida et al. (2014). [Note that since Koshida et al. (2014) studied variable but non-periodic AGN, nor is the Doppler-boosted lighthouse model likely appropriate for their single black hole systems, their work does not suffer the same degeneracy with integer multiples of the variability period.] The *WISE* $W1$ and $W2$ filters correspond to rest-frame 2.6 and $3.6\mu\text{m}$ at $z = 0.278$. Using the median optical magnitudes of $V \simeq R \simeq 15.0$, the rest-frame V -band luminosity of PG 1302-102 is $L_V \simeq 6.56 \times 10^{45} \text{ erg s}^{-1}$. Based on the K -band $R_{\text{dust}} - L$ relation (Koshida et al. 2014), the expected observed-frame time lag at $z = 0.278$ is $\tau \simeq 1590 \pm 150$ days. Our $W1$ and $W2$ lags are above the Koshida et al. (2014) relation by 0.15 and 0.18 dex for $n = 1$, and 0.41 and 0.43 dex for $n = 2$. The former offsets are comparable to the observed scatter of the relation (0.14 dex), but the latter are not, consistent with the $T/2$ delay effect and the large inclination angle required by the lighthouse model. We also note that the K -band $R_{\text{dust}} - L$ relation generally predicts R_{dust} smaller than R_{sub} by factors of a few, and Koshida et al. (2014) details how R_{sub} depends both on dust grain size and the details of the dust grain absorption efficiency. Also, Nenkova et al. (2008) note that the largest grains could survive to closer radii than R_{sub} , presumably detected by the K -band time lags.

Previous near-infrared studies of local AGN have shown dust lags are typically longer at longer near-infrared wave-

lengths, since cooler material (e.g., further out material) will dominate the emission at progressively longer wavelengths (e.g., Kishimoto et al. 2011b; Vazquez et al. 2015). The $W2$ time lag is consistent with, or only marginally larger than the $W1$ lag with a ratio 1.09 ± 0.10 for the $n = 1$ and 1.05 ± 0.05 for the $n = 2$ solution in equation (1). Following Vazquez et al. (2015), we quote the radial distribution of dust grains in radiative equilibrium (e.g., Barvainis 1987; Nenkova et al. 2008) scaling with temperature as $R_{\text{dust}} \sim T^{-2.6}$ and find $R_{\text{dust},W2}/R_{\text{dust},W1} \simeq 2.3$, much higher than the value from this study. Alternative explanations such as clumpy tori (Nenkova et al. 2008) are successful in emitting a broad infrared spectrum from a confined distribution of dust.

4. DISCUSSION

Graham et al. (2015ab) list several possible physical mechanisms to produce the periodic optical light curves in PG 1302-102: non-thermal contribution from a precessing jet in a supermassive black hole binary, periodic mass accretion in a circumbinary accretion disk, or a precessing warped disk (which might also be related to a binary supermassive black hole). Our results suggest that the observed mid-infrared variability is being driven by variations in the accretions disk(s). For example, in the precessing jet scenario, one would expect very little temporal offsets, if any, between the optical and infrared variability. Indeed, the observed periodic signal in the *WISE* data and the cross correlation results support that dust is reverberating input luminosity from the accretion disk.

The elliptical host galaxy morphology of PG 1302-102 and the presence of close companion galaxies around it (Bahcall et al. 1995; Disney et al. 1995) are suggestive of a recent merger driving high-luminosity AGN activity (e.g., Treister et al. 2012; Hong et al. 2015). Indeed, the host galaxy of PG 1302-102 measured from H - and R -band imaging are classified as asymmetric and tidal tail morphologies, respectively (Guyon et al. 2006; Hong et al. 2015). The galaxy-scale morphology hints that this system may be in an ongoing merger.

The mid-infrared light curves of PG 1302-102 are indicative of periodic dust reverberation lagging behind the optically periodic light curve due to the light travel time to the mid-infrared emitting dusty torus, with a possible additional phase lag in the relativistic Doppler boosting lighthouse model. For both models, the time lags imply that the dust is echoing outside the accretion disk but from a small, possibly clumpy medium, and we predict that the narrow fluorescent Fe $K\alpha$ X-ray emission should vary on the same period and with the same phase lag as the mid-infrared emission. Time domain studies are starting to reveal events in AGNs occurring on physical scales that are not resolvable from the Earth, helping to constrain the source of variability and properties of the variable structure (e.g., Risaliti et al. 2013; LaMassa et al. 2015; Mehdipour et al. 2015; Stern et al. 2015). In particular, multiwavelength time domain surveys of AGN combining optical data with mid-infrared data from *WISE*, as done here, or from the *Spitzer Space Telescope* (e.g., Gorjian et al. 2014; Vazquez et al. 2015), probe the physical structure and accretion mechanisms of the AGN accretion disk and surrounding dusty material.

We thank the anonymous referee for the comments which greatly improved the paper, as well as Daniel D’Orazio, Moshe Elitzur, Saavik Ford, Zoltan Haiman, Barry McK-

nan, and Robert Nikutta for helpful discussions. This research was supported by an appointment to the NASA Postdoctoral Program at the Jet Propulsion Laboratory, administered by Oak Ridge Associated Universities through a contract with NASA. This publication makes use of data products from the *Wide-field Infrared Survey Explorer*, which is a joint project of the University of California, Los Angeles, and the Jet Propulsion Laboratory/California Institute of Technology, funded by the National Aeronautics and Space Administration. This publication makes use of data products from *NEOWISE*, which is a project of the Jet Propulsion Laboratory/California Institute of Technology. *NEOWISE* is funded by the National Aeronautics and Space Administration. CRTS was supported by the NSF grants AST-1313422 and AST-1413600. DS acknowledges support from NASA through ADAP award 12-ADAP12-0109.

Facilities: CRTS, WISE, NEOWISE

©2015. All rights reserved.

REFERENCES

- Bahcall, J. N., Kirhakos, S., & Schneider, D. P. 1995, *ApJ*, 450, 486
 Barvainis, R. 1987, *ApJ*, 320, 537
 Bentz, M. C., Peterson, B. M., Pogge, R. W., Vestergaard, M., & Onken, C. A. 2006, *ApJ*, 644, 133
 Blandford, R. D., & Payne, D. G. 1982, *MNRAS*, 199, 883
 Clavel, J., Wamsteker, W., & Glass, I. S. 1989, *ApJ*, 337, 236
 Disney, M. J., Boyce, P. J., Blades, J. C., et al. 1995, *Nature*, 376, 150
 D’Orazio, D. J., Haiman, Z., & MacFadyen, A. 2013, *MNRAS*, 436, 2997
 D’Orazio, D. J., Haiman, Z., Duffell, P., Farris, B. D., & MacFadyen, A. I. 2015a, *MNRAS*, 452, 2540
 D’Orazio, D. J., Haiman, Z., & Schiminovich, D. 2015b, *Nature*, 525, 351
 Drake, A. J., Djorgovski, S. G., Mahabal, A., et al. 2009, *ApJ*, 696, 870
 Gorjian, V., Barth, A. J., Bloom, J. S., et al. 2014, *American Astronomical Society Meeting Abstracts #223*, 223, #251.08
 Graham, M. J., Djorgovski, S. G., Drake, A. J., et al. 2014, *MNRAS*, 439, 703
 Graham, M. J., Djorgovski, S. G., Stern, D., et al. 2015a, *Nature*, 518, 74
 Graham, M. J., Djorgovski, S. G., Stern, D., et al. 2015b, *MNRAS*, 453, 1562
 Guyon, O., Sanders, D. B., & Stockton, A. 2006, *ApJS*, 166, 89
 Hong, J., Im, M., Kim, M., & Ho, L. C. 2015, *ApJ*, 804, 34
 Horne, J. H., & Baliunas, S. L. 1986, *ApJ*, 302, 757
 Jun, H. D., & Im, M. 2013, *ApJ*, 779, 104
 Jun, H. D., Im, M., Lee, H. M., et al. 2015, *ApJ*, 806, 109
 Kaspi, S., Smith, P. S., Netzer, H., et al. 2000, *ApJ*, 533, 631
 Kishimoto, M., Hönig, S. F., Antonucci, R., et al. 2011a, *A&A*, 527, A121
 Kishimoto, M., Hönig, S. F., Antonucci, R., et al. 2011b, *A&A*, 536, A78
 Koshida, S., Minezaki, T., Yoshii, Y., et al. 2014, *ApJ*, 788, 159
 LaMassa, S. M., Cales, S., Moran, E. C., et al. 2015, *ApJ*, 800, 144
 Liu, T., Gezari, S., Heinis, S., et al. 2015, *ApJ*, 803, L16
 MacLeod, C. L., Ivezić, Ž., Sesar, B., et al. 2012, *ApJ*, 753, 106
 Mainzer, A., Bauer, J., Cutri, R. M., et al. 2014, *ApJ*, 792, 30
 Marziani, P., Sulentic, J. W., Dultzin-Hacyan, D., Calvani, M., & Moles, M. 1996, *ApJS*, 104, 37
 Mehdipour, M., Kaastra, J. S., Kriss, G. A., et al. 2015, *A&A*, 575, 22
 Nenkova, M., Sirocky, M. M., Nikutta, R., Ivezić, Ž., & Elitzur, M. 2008, *ApJ*, 685, 160
 McLure, R. J., & Jarvis, M. J. 2002, *MNRAS*, 337, 109
 Mor, R., & Netzer, H. 2012, *MNRAS*, 420, 526
 Murakami, H., Baba, H., Barthel, P., et al. 2007, *PASJ*, 59, 369
 Ohya, Y., Onaka, T., Matsuhara, H., et al. 2007, *PASJ*, 59, 411
 Ojha, R., Zacharias, N., Hennessy, G. S., Gaume, R. A., & Johnston, K. J. 2009, *AJ*, 138, 845
 Oknyanskij, V. L., & Horne, K. 2001, *Probing the Physics of Active Galactic Nuclei*, 224, 149
 Penston, M. V., Penston, M. J., Selmes, R. A., Becklin, E. E., & Neugebauer, G. 1974, *MNRAS*, 169, 357
 Peterson, B. M. 1993, *PASP*, 105, 247
 Peterson, B. M., Wanders, I., Horne, K., et al. 1998, *PASP*, 110, 660
 Prochaska, J. X., Weiner, B., Chen, H.-W., Cooksey, K. L., & Mulchaey, J. S. 2011, *ApJS*, 193, 28
 Richards, G. T., Lacy, M., Storrie-Lombardi, L. J., et al. 2006, *ApJS*, 166, 470
 Risaliti, G., Harrison, F. A., Madsen, K. K., et al. 2013, *Nature*, 494, 449
 Shi, J.-M., Krolik, J.H., Lubow, S.H. & Hawley, J.F. 2012, *ApJ*, 749, 118
 Suganuma, M., Yoshii, Y., Kobayashi, Y., et al. 2006, *ApJ*, 639, 46
 Stern, D., Arav, N., Graham, M. J. et al. 2015, *ApJ*, submitted
 Swain, M., Vasisht, G., Akeson, R., et al. 2003, *ApJ*, 596, L163
 Treister, E., Schawinski, K., Urry, C. M., & Simmons, B. D. 2012, *ApJ*, 758, L39
 Vazquez, B., Galianni, P., Richmond, M., et al. 2015, *ApJ*, 801, 127
 Vestergaard, M., & Peterson, B. M. 2006, *ApJ*, 641, 689
 Wright, E. L., Eisenhardt, P. R. M., Mainzer, A. K., et al. 2010, *AJ*, 140, 1868